

PREDICTIONS FOR THE CORRELATION BETWEEN GIANT AND TERRESTRIAL EXTRASOLAR PLANETS IN DYNAMICALLY EVOLVED SYSTEMS

DIMITRI VERAS^{1,2} AND PHILIP J. ARMITAGE^{1,2}

ApJ, in press

ABSTRACT

The large eccentricities of many giant extrasolar planets may represent the endpoint of gravitational scattering in initially more crowded systems. If so, the early evolution of the giant planets is likely to be more restrictive of terrestrial planet formation than would be inferred from the current, dynamically quiescent, configurations. Here, we study statistically the extent of the anti-correlation between giant planets and terrestrial planets expected in a scattering model. We use marginally stable systems of three giant planets, with a realistic range of planetary masses, as a simple model for the initial conditions prior to scattering, and show that after scattering the surviving planets reproduce well the known extrasolar planet eccentricities beyond $a > 0.5$ AU. By tracking the minimum periastron values of all planets during the evolution, we derive the distribution of orbital radii across which strong perturbations (from crossing orbits) are likely to affect low mass planet formation. We find that scattering affects inner planet formation at orbital separations less than 50% of the final periastron distance, q_{fm} , of the innermost massive planet in approximately 30% of the realizations, and can occasionally influence planet formation at orbital separations less than 20% of q_{fm} . The domain of influence of the scattering massive planets increases as the mass differential between the massive planets decreases. Observational study of the correlation between massive and terrestrial extrasolar planets in the same system has the potential to constrain the origin of planetary eccentricity.

Subject headings: solar system: formation — planets and satellites: formation — planetary systems: formation — celestial mechanics

1. INTRODUCTION

Studies of the population of small bodies – comets, asteroids, and Kuiper belt objects – have provided powerful constraints on the early dynamical evolution of the massive planets in the Solar System. The concentration of objects in the outer Solar System in narrow zones in resonance with Neptune, with significant eccentricities, provides evidence for an early expansion of Neptune’s orbit (Malhotra 1995; Hahn & Malhotra 1999; Murray-Clay & Chiang 2005), and has motivated a scenario in which the orbits of Saturn, Uranus and Neptune all expanded as a consequence of scattering the planetesimal debris left over after planet formation (Thommes, Duncan & Levison 1999, 2002; Tsiganis et al. 2005). Migration of Jupiter – albeit for a much smaller distance – is also predicted within such models and may have left its own signature in the distribution of Hilda asteroids (Franklin et al. 2004).

There is no near or medium term prospect for obtaining observations that would permit directly comparable studies in extrasolar planetary systems. A wealth of circumstantial evidence, however, suggests that the early evolution of many extrasolar planetary systems may have been more stochastic than in the Solar System, and these more dramatic histories *can* be investigated by studying the relationship between terrestrial planets (which are here being utilized purely as test particles of negligible mass) and giant planets within the same system. The space-based tran-

sit mission *Kepler* (Basri, Borucki & Koch 2005) will offer the first definite opportunity to conduct such investigations, though terrestrial planets may also be discovered via giant planet transit timing techniques (Agol et al. 2005; Holman & Murray 2005) or high-precision astrometry with the *Space Interferometry Mission* (Ford & Tremaine 2003). Gravitational microlensing also has potential for terrestrial planet discovery (Bennett & Rhie 2002), although the prospects for determining the overall architecture of systems in which planets are discovered are poor with this method.

High eccentricities have become a common signature of known extrasolar planets which reside outward of the tidal circularization limit. The origin of these eccentricities remains unclear. Further, Goldreich, Lithwick & Sari (2004) have suggested that the giant planets in the Solar System might have experienced large eccentricities before becoming circularized to their present values. One popular model attributes the eccentricity to gravitational scattering among multiple massive planets (Rasio & Ford 1996; Lin & Ida 1997; Levison, Lissauer & Duncan 1998; Ford, Rasio & Yu 2003; Marzari & Weidenschilling 2002). Scattering simulations have produced a quantitative match to the distribution of known extrasolar planet eccentricities (Ford, Rasio & Yu 2003), and can also explain the current configuration of the upsilon Andromedae system (Ford, Lystad & Rasio 2005). However, we cannot rule out the possibility that protoplanetary disk physics allows planetary eccentricity to be excited via the interaction between a *single* massive planet and a gas disk (Artymowicz et al. 1991; Papaloizou, Nelson & Masset 2001; Ogilvie & Lubow 2003; Goldreich & Sari 2003).

These two models for eccentricity growth have differ-

¹ JILA, Campus Box 440, University of Colorado, Boulder CO 80309-0440; dimitri.veras@colorado.edu; pja@jilau1.colorado.edu

² Department of Astrophysical and Planetary Sciences, University of Colorado, Boulder CO 80309-0391

ent consequences for the formation of terrestrial planets within the same system. If eccentricity arises from planet-disk interactions, then an eccentricity comparable to the final value is likely to be established soon after the formation of the giant planet, which must occur prior to the dissipation of the gas disk during the first few Myr (Haisch, Lada & Lada 2001). This schedule probably precedes the final stages of terrestrial planet formation. Chambers & Cassen (2002), Levison & Agnor (2003) and Mardling & Lin (2004) have studied in detail the effect of the giant planet configuration, and its evolution, on the formation of terrestrial planets. If, conversely, eccentricity is the endpoint of gravitational scattering among several massive planets, then the dynamics involved in the scattering process will usually involve multiple rearrangements of the planets prior to stabilization (usually by ejection) and establishment of a ‘final’ configuration. The extent of the ejection is dependent on the masses, radii, and initial orbital separations of the planets. During such rearrangements, which can take many Myr, giant planets can temporarily intrude (either physically, or via their resonances) into the terrestrial planet zone. The resulting constraints on where terrestrial planets can form and survive are bound to be more restrictive than those calculated assuming that the current observed (i.e. final) configuration of massive planets has existed for all time (Jones, Sleep & Chambers 2001; Menou & Tabachnik 2003; Asghari et al. 2004; Ji et al. 2005).

In an earlier paper (Veras & Armitage 2005), we investigated whether massive planet scattering - while producing final dynamically settled states that admit stable terrestrial planets - might prevent terrestrial planets from surviving the transition to those states. Using test particles to follow explicitly the evolution of material (either formed terrestrial planets, or planetary embryos) in the terrestrial planet zone, we concluded from a limited number of realizations that there were circumstances in which the scattering process would impede subsequent planet formation at small radii. The dominant process for removing test particles was physical intrusion of a giant planet into the terrestrial planet region - i.e. the temporary existence of crossing orbits.

In this paper, we quantify statistically the extent of the anti-correlation which massive planet scattering should introduce between the presence of massive and terrestrial planets in the same system. We assume, based on our previous results (Veras & Armitage 2005), that terrestrial planet formation will be strongly suppressed exterior to the minimum periastron distance attained by any giant planet during the dynamical evolution, and calculate this minimum periastron distance from an ensemble of 500 N-body simulations. The appropriate initial conditions for scattering experiments are uncertain - here we assume that the initial states are triple planet point mass systems in which the planets have a realistic range of masses (Tabachnik & Tremaine 2002). Although undoubtedly oversimplified, these initial conditions lead to final states which match the observationally determined eccentricity distribution of exoplanets reasonably well.

The outline of this paper is as follows. Section §2 describes the motivation behind our initial conditions, and section §3 briefly describes the numerical codes used. We describe our results in §4, and discuss some of the impli-

cations in §5.

2. INITIAL CONDITIONS

A large number of different initial configurations of massive planets are likely to evolve, via gravitational scattering, toward stable arrangements that match the observed eccentricity distribution of extrasolar planets. Massive planet formation theory does not provide any clear guidance as to the expected distribution of the number of planets that would be formed in a single system, so it is reasonable to adopt any number from $N = 2$ (Rasio & Ford 1996) to large N (Papaloizou & Terquem 2001). That said, for simulations that ignore gas (as ours do), it is desirable for internal consistency to choose initial conditions that yield instability on a timescale comparable to, or longer than, the dispersal timescale of the gaseous protoplanetary disk. Wolk & Walter (1996) estimate this timescale observationally to be $\lesssim 10^5$ yr, although it is not well constrained. Unfortunately many setups do in fact yield a significant fraction of rapidly unstable initial conditions (for example Holman & Wisdom (1993) find a logarithmic decay of the number of surviving test particles in an outer Solar System simulation), though it is possible to at least avoid extremely short (and thus grossly inconsistent) instability timescales. Here, we model systems of three giant planets, with the motivation being that they represent the simplest systems which yield instability on the desired timescale without considerable fine-tuning of the initial planetary separations.

2.1. Initial planetary separations

Chambers, Wetherill & Boss (1996) and Marzari & Weidenschilling (2002) plot dynamical settling times for three-planet systems as functions of initial separations, while Ito & Tanikawa (2001) show similar plots for sets of 9 and 14 terrestrial-like planets which are perturbed by Jupiter and Saturn. The instability timescales for the three-planet systems exhibit an exponential dependence on initial separations, but were based on constant initial planetary separations and equal mass planets, simplifications not assumed in this work. Hence, although we used such diagrams as guidelines for establishing our initial conditions, we performed trial simulations of in order to determine the appropriate instability times for our runs. Based on those runs, we fixed our initial inner, middle, and outer planet semimajor axes at $a_1 = 5$ AU, $a_2 = 6$ AU, and $a_3 = 12$ AU respectively. The ratio of semimajor axes for the inner pair of planets, $a_2/a_1 = 1.2$, lies just within the globally chaotic limit established by Wisdom (1980) for two-planet systems. Typically, these semimajor axis choices produce instability that causes the ejection of at least one planet on timescales exceeding several orbits but less than several million years. The system dynamically settles to a state that at least qualitatively resembles known multiplanet exosystems - often one featuring two well-separated eccentric giant planets.

Since we ignore physical collisions between giant planets, our simulations are freely scalable - only the ratios, and not the magnitudes, of a_1, a_2, a_3 have physical significance. Nevertheless, our choices are plausible, since giant planet formation close (within a few AU) to a star is unlikely, while the predicted timescale for planet for-

mation via core accretion (Pollack et al. 1996) does not vary dramatically for $a \approx 5 - 10$ AU.

2.2. Masses

Simulations of gravitational scattering within two-planet systems show that the results are dependent on the assumed mass distribution (Rasio & Ford 1996; Ford, Rasio & Yu 2003). Here, we randomly assigned masses to each giant planet in the range from $0.3M_{Jup}$ to $3M_{Jup}$, weighed by the $1/M$ power-law distribution determined by Tabachnik & Tremaine (2002). This range, the lower bound of which represents a Saturn mass, covers one order of magnitude, and accounts for the majority of exoplanet minimum masses so far discovered. Our mass distribution is weighted toward subjovian masses in order to mirror the actual distribution of exoplanet masses. We note that we do not account for possible systematic differences between the mass distribution at formation, and that determined observationally following (within this model) gravitational scattering, which typically ejects lower mass planets more frequently than high mass planets. Nor do we consider correlations between semimajor axis and mass at the epoch of formation.

2.3. Eccentricities and inclinations

Having determined the initial separations and masses of the giant planets, we randomized each planet’s angular variables for each run. Each planet initially resides on a near-circular orbit, with an eccentricity of 0.01, and a random and negligible, but nonzero, inclination, of less than 0.001° . Such near-zero eccentricity and inclination values are similar to those used by Ford, Rasio & Yu (2003) in their two-planet simulations. We fix our initial values so as not to introduce additional variables which should be considered when analyzing the results. Regardless, the variance in Ford, Rasio & Yu (2003)’s initial eccentricity and inclination values do not appear to drastically alter their results.

3. NUMERICAL METHOD

We ran the scattering experiments using two independent gravitational N-body codes. Our primary tool was the HNbody code (K. P. Rauch & D. P. Hamilton 2006, in preparation). HNBody is a collection of integrators primarily designed for systems with one massive central object, and has been used for both massive extrasolar planet simulations (Veras & Armitage 2004a,b, 2005) and satellite interactions around Neptune (Zhang & Hamilton 2005). As a check, we also ran experiments with a Hermite stellar dynamics code (Hut & Makino 2003), which, although not as efficient as HNbody for this problem, is perfectly able to evolve systems for the relatively modest durations of our simulations. Adjustable run-time parameters for HNbody include choice of integrator, accuracy parameter, and timestep, whereas only timestep is a required parameter for the Hermite code. Given the Bulirsch-Stoer integrator’s ability to model accurately close encounters between planets, we chose this integrator for all HNbody simulations. The user-inputted timestep then sets the maximum timestep over which the integrator may iterate while still maintaining a pre-specified accuracy. We used a timestep of 0.025 yr, which corresponds to a robust 1/200 of an orbit of the initially innermost planet (note

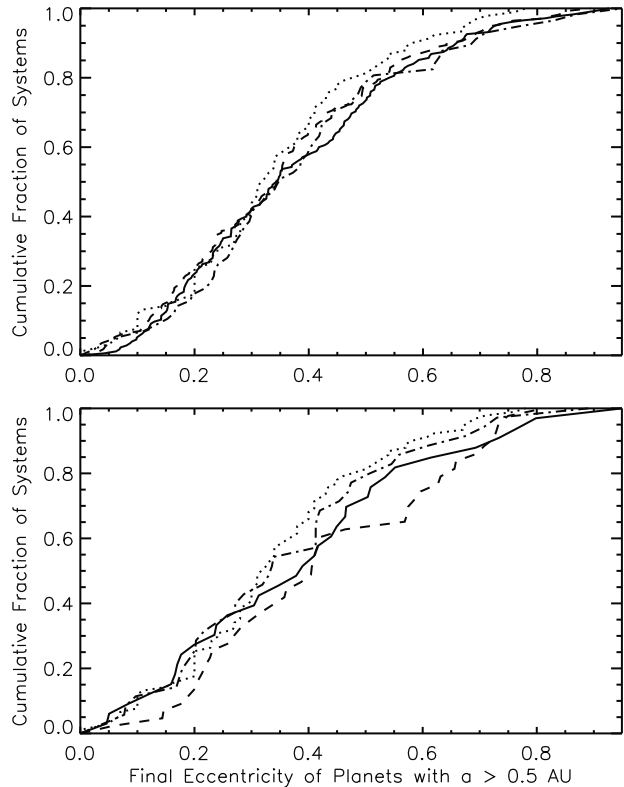


FIG. 1.— The cumulative distribution of the observed extrasolar planet eccentricities beyond $a > 0.5$ AU (dotted lines) and the simulated distribution from the HNbody (solid lines) and Hermite (dashed lines) codes for 5 Myr simulations (upper panel) and 10 Myr simulations (lower panel). The dot-dashed lines represents an additional simulated HNbody distribution derived from a different set of initial EGP semimajor axes of 5, 10, and 12 AU.

that during the evolution, a for the innermost planet can decrease substantially, so a large safety margin at the start of the evolution is necessary). The resulting relative energy errors were $\sim 10^{-9} - 10^{-12}$ throughout the simulation. For the Hermite code, we chose a smaller timestep of 1/1000 of an orbit for the innermost planet, as the code is not specialized for planetary problems. Even with the reduction in timestep, the relative errors ($\sim 10^{-4} - 10^{-6}$) are orders of magnitude larger than those from the HNbody code, but still acceptable. Data was outputted at every 250-500 yr depending on the simulation.

In order to maximize the number of relevant simulations run while maintaining acceptable standards of energy conservation, we performed a suite of preliminary tests. As the chaotic nature of the unstable systems we analyzed produces different evolutionary tracks due to machine-precision roundoff error, we do not compare simulations run with both codes on an individual basis. Rather, we perform a statistical comparison. We are also interested in comparing the distribution of final planetary eccentricities with observations, and for this purpose we consider only exoplanets with semimajor axes > 0.5 AU; closer planets could have been influenced by tidal effects, which were not modeled by our simulations. We also only compare planets in systems in which dynamical instability produced crossing orbits, leaving only one or

TABLE 1
KS TEST NUMBERS FOR ECCENTRICITY
DISTRIBUTIONS

	5 Myr runs	10 Myr runs
actual-HNbody#1	13.8%	36.0%
actual-Hermite	71.5%	57.6%
HNbody#1-Hermite	41.0%	46.6%
HNbody#2-HNbody#1	88.3%	96.0%
HNbody#2-Hermite	75.0%	22.9%
HNbody#2-actual	75.6%	41.2%

NOTE. — The KS test probability that different pairs of distributions, plotted in Figure 1, are actually drawn from the same parent distribution. The designation “HNbody #2” represents the additional simulation run with initial EGP semimajor axes of 5, 10, and 12 AU. All four distributions are broadly consistent.

two planets in stable orbits. Over half of the systems modeled with our initial conditions produced such instability.

4. RESULTS

For our main sample, we evolved 250 systems using HNbody for 5 Myr. This duration is comparable (in terms of orbits) to several previous studies (Ford, Havlickova & Rasio 2001; Adams & Laughlin 2003; Veras & Armitage 2004a). Of these runs, 243 achieved crossing orbits, and 175 exhibited at least one planet achieving a hyperbolic orbit. We also ran 250 Hermite 5-Myr simulations, 244 of which achieved crossing orbits, and 170 of which exhibited at least one planet achieving hyperbolic orbits. No planet which remained stable throughout our simulations evolved its semimajor axis to within a region where tidal effects would become important. Therefore, we did not need to incorporate tidal corrections into the statistical comparisons. Although with our initial conditions significant dynamical evolution frequently occurs within 5 Myr, it is by no means obvious that the ultimate dynamical state is attained within this period. Hence, we carried out a smaller set of 50 10-Myr simulations with each integrator in order to check whether this alters the qualitative or quantitative results; we present results from both sets of simulations concurrently. The planets in all such simulations achieved crossing orbits. The number of systems which achieved hyperbolic orbits for the HNbody and Hermite simulations were 33 and 43 respectively. We only consider systems in which one or more planet has been ejected.

Figure 1 displays the 91 known extrasolar planet eccentricities as of June 1st, 2005 which satisfy $a \geq 0.5$ (dotted line), along with the final eccentricity distributions of the surviving planets from the 5 Myr (upper panel) and 10 Myr (lower panel) HNbody (solid line) and Hermite (dashed line) simulations. The HNbody distributions from a different set of initial EGP conditions, where $a_1 = 5$ AU, $a_2 = 10$ AU, and $a_3 = 12$ AU, are superimposed on both panels as dash-dot lines. Respectable agreement is obtained, both between the results from the two numerical codes, and between the simulations and the observed distribution of eccentricities of

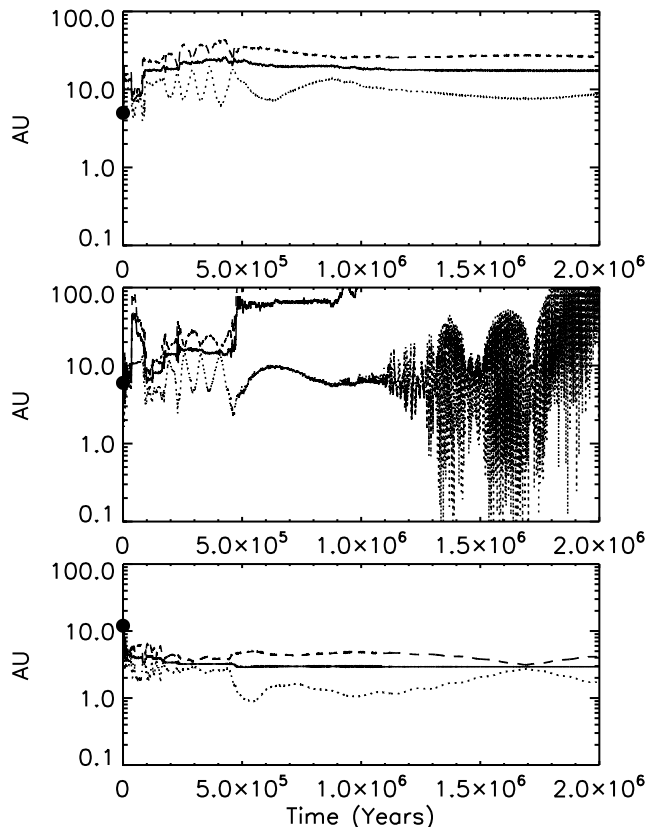


FIG. 2.— Evolution of the semimajor axis (solid lines), periastron (dotted lines), and apoastron (dashed lines) of the three planets for a single run. In this case, the planet with $a_2 = 6$ AU at $t = 0$ (middle panel) was eliminated from the system. The eliminated EGP performs a nearly complete radial sweep of the system between 1.5 and 2 Myr.

extrasolar planets. Quantitatively, a KS test (Table 1) verifies that the simulated and observed eccentricities are consistent with their being drawn from the same parent distribution. This agreement may be somewhat fortuitous, especially at the high e end of the distribution, where the observed population may have been underestimated due to selection effects (Cumming 2004). Less than 2% of the planets simulated in this work attain eccentricities higher than 0.8, the upper eccentricity limit predicted by Ford, Rasio & Yu (2003) for the two-planet scattering model in which both planets initially reside on coplanar, circular orbits. The occasional higher eccentricity values found in this study may be attributed to the four-body nature of the system and the small ($= 0.01$) nonzero initial EGP eccentricity values.

The agreement demonstrated in Figure 1 suggests that our simulations yield outcomes that are consistent with the dynamical properties of actual systems. Of course this agreement is in no way unique, and other scattering scenarios are known that produce similar results. For example, we obtain rather similar results to those of Ford, Rasio & Yu (2003), despite substantially different initial conditions. A range of masses among the scattering planets does appear to be important.

Within our model, the effective sphere of influence of the giant planets on subsequent terrestrial planet formation is dictated by the radial excursions of the giant

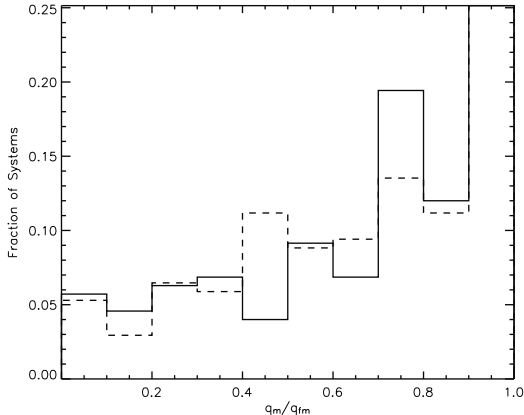


FIG. 3.— The distribution of the ratio q_m/q_{fm} after 5 Myr, where q_m is the minimum periastron distance achieved by any planet throughout the simulation, and q_{fm} is the minimum periastron among the surviving planets at the final state of the simulation. HNbody simulations are represented by solid lines and Hermite simulations are represented by dashed lines.

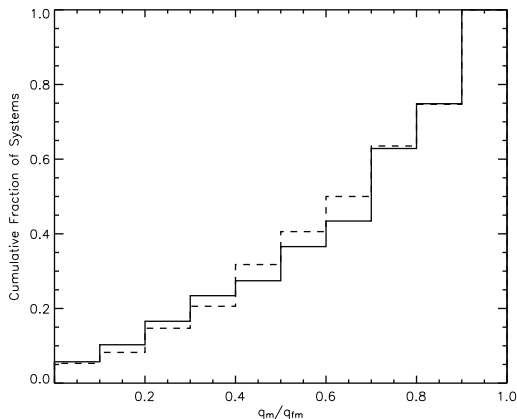


FIG. 4.— The cumulative distribution of the ratio q_m/q_{fm} after 5 Myr, where q_m is the minimum periastron distance achieved by any planet throughout the simulation, and q_{fm} is the minimum periastron among the surviving planets at the final state of the simulation. HNbody simulations are represented by solid lines and Hermite simulations are represented by dashed lines.

planets during their dynamical evolution. Since dynamical instability often causes crossing orbits, the most restrictive conditions (i.e. the greatest inward excursions) can be set by any of the initial three planets. One example is depicted in Figure 2, which shows the evolution of the semimajor axis, pericenter and apocenter of the three planets for the first 2 Myr of a 5 Myr run. In this case, the final state of the system leaves two planets in moderately eccentric, well-separated periodic orbits. However, in the evolution up to this state, the initially innermost and outermost planets switched positions, while the third planet swept radially through the entire system within 2 Myr, and harbored a pericenter which remained close to the parent star for nearly 0.5 Myr. This behavior is effectively hidden by the benign final state of the system.

In order to quantify how common such evolutionary histories are, we consider the ensemble of simulations discussed above. We denote by q_m the minimum periastron distance achieved by any planet throughout the

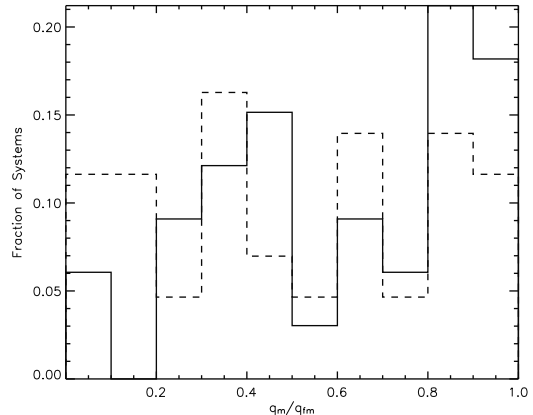


FIG. 5.— The distribution of the ratio q_m/q_{fm} after 10 Myr, where q_m is the minimum periastron distance achieved by any planet throughout the simulation, and q_{fm} is the minimum periastron among the surviving planets at the final state of the simulation. HNbody simulations are represented by solid lines and Hermite simulations are represented by dashed lines.

simulation, and by q_{fm} the minimum periastron among the surviving planets at the termination of the simulation. Figure 3 shows the distribution of the ratio of these distances, q_m/q_{fm} , for the 5 Myr HNbody (solid line) and Hermite (dashed line) simulations respectively. Figure 4 is the corresponding set of cumulative histograms. We find, as previously (Veras & Armitage 2005), that the periastron distance for the innermost planet in the final, relaxed state, is often a poor proxy for the extent of radial sweeping that occurs during the earlier dynamical evolution. Although q_m/q_{fm} does increase toward $q_m/q_{fm} = 1$, the distribution is broad and extends down to quite small values $q_m/q_{fm} \lesssim 0.2$. From the cumulative histograms, we find that $q_m/q_{fm} \lesssim 0.2$ in approximately 10% of realizations, while $q_m/q_{fm} \lesssim 0.5$ in approximately 30% of cases. Within a scattering scenario, we would therefore expect to observe a significant deficit of lower mass planets in orbits with semimajor axes less than half the periastron distance of the innermost massive planet. Many orbits in this exclusion zone would be stable today, but would have been unfavorable for planet formation due to the early massive planet dynamics. No significant difference between results computed with the two codes is seen. Broadly similar results are also obtained from the simulations run on for 10 Myr – plotted in Figure 5 – albeit with poorer statistics.

No simulations so far described include terrestrial planets. As a further demonstration of our results and as a check on the approximate criterion for strong interactions adopted earlier, we performed 7 additional simulations including 50 terrestrial planets over 5 Myr with HNbody. The planets were treated as “Light Weight Particles” (LWPs), which are test particles that do not perturb EGP. The LWPs were initially placed uniformly in annuli ranging from 0.5 – 1.5 AU (2 simulations) or 1.0 – 3.0 AU (5 simulations) on circular, nearly coplanar orbits. Figure 6 provides a snapshot of the final states of all 7 simulations, with dots representing surviving LWPs, solid lines representing q_m , and dotted lines enclosing the initial LWP annulus. The plots are arranged according to decreasing q_m in order to illustrate

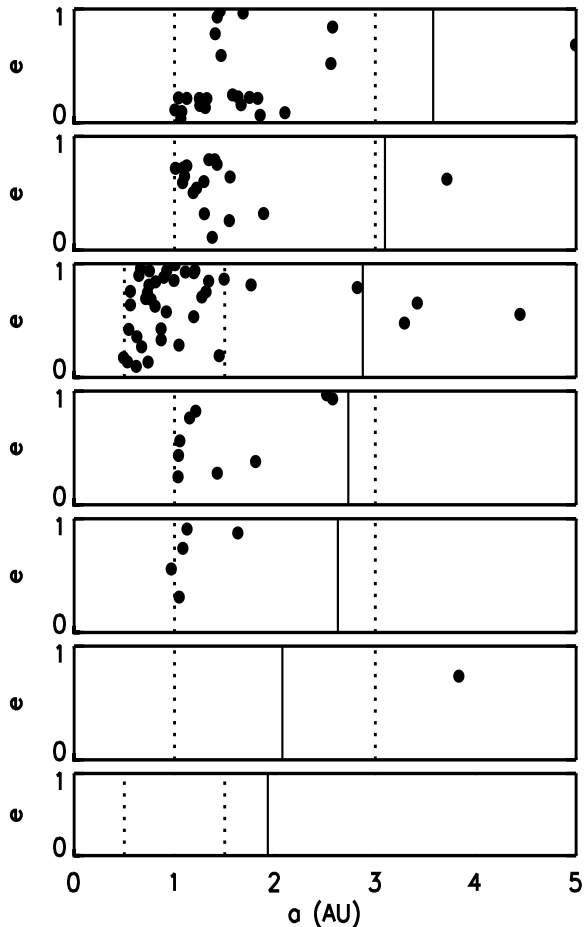


FIG. 6.— Final states, after 5 Myr, of 7 simulations each run with 3 EGPs and 50 terrestrial planets, where dots denote surviving terrestrial planets, dotted lines enclose the initial semimajor axes of those planets, and solid lines denote q_m , the minimum periastron distance achieved by any EGP throughout the simulation. Two different initial terrestrial planet annuli are sampled.

just how sensitively terrestrial planet survival depends upon EGP excursion into the inner system. These runs show that although occasionally low mass bodies may survive with semi-major axes outside the minimum periastron separation, typically there’s significant clearing even within the minimum periastron distance. Hence, the approximate criteria we’ve adopted is on the conservative side. The uppermost panel indicates that the initially low eccentricities of LWPs will remain near-circular if the EGPs fail to intrude upon a region within twice the radial distance of the terrestrial material; the seemingly anomalous vertical band of LWPs at ≈ 1.3 AU may be attributed to strong resonant interactions with the approaching EGPs.

The random planet mass distribution used in the simulations raises an additional question – which combinations of planet masses promote the greatest extent of radial sweeping? Under some circumstances (for example when two planets remain on stable bound orbits at the end of the evolution), clues as to the initial masses of the scattering planets may survive the scattering process, so any strong correlation between the masses and the outcome is potentially observable. Figure 7 shows how the mean q_m scales with the range of planet masses

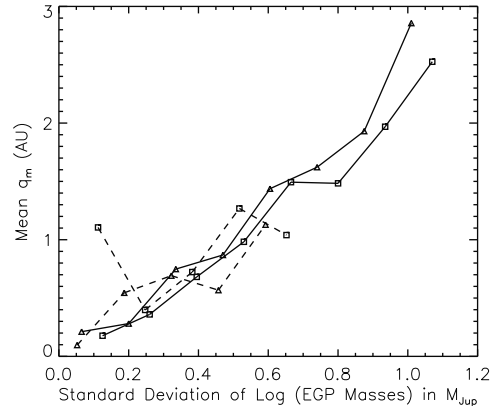


FIG. 7.— Variation of the mean q_m values with the variance of the initial planet masses, for 5 Myr (solid line) and 10 Myr (dashed line) simulations using the HNbody (triangles) and Hermite (squares) codes. Plotted points refer to binned values of the logged mass standard deviation. Masses were randomly sampled from a $1/M$ distribution.

in the randomly chosen initial conditions, quantified via the standard deviation of the log of the planet masses. In the figure, solid lines denote the 5 Myr simulations, dashed lines indicate 10 Myr simulations, and triangles and squares refer, respectively, to the HNbody and Hermite code simulations. We find a roughly linear trend – as the scatter in the mass increases, so does the mean value of q_m . Systems in which the planets are of roughly similar masses are therefore most detrimental to the survival of interior terrestrial planet material. Given our assumed $1/M$ distribution of masses, we expect EGP standard mass deviations of over $1M_{Jup}$ to be relatively rare.

Within our assumed scattering scenario for the origin of extrasolar planet eccentricities, the extent of the penetration of giant planets into the terrestrial planet zone is likely to be the dominant factor determining whether the evolution hinders subsequent terrestrial planet formation. However, the amount of time spent with giant planets at small periastron distances may also be significant. We find a wide gap between the timescale on which crossing orbits first develop, and the timescale on which a planet is first forced onto a hyperbolic orbit. Crossing orbit times for our simulations are on the order of 10^3 yr – short enough that the effects of a residual decaying gas disk would obviously be important and modify the result. By contrast, the timescale for ejections is of the order of a Myr. Figure 8 is a histogram of the initial time on which a planet achieves a hyperbolic orbit in the 5 Myr simulations for the HNbody (solid line) and Hermite (dashed line) simulations. Because the timescales on which planetary orbits merely cross versus become hyperbolic vary by several orders of magnitude, Saturn or Jovian-mass planets may be dynamically excited for hundreds of thousands of years before being ejected from the system, suffering a collision, or dynamically settling into a quasi-stable configuration such as that in Figure 2. Intrusions into the terrestrial planet zone are therefore typically repeated and / or extended, rather than being one-time events.

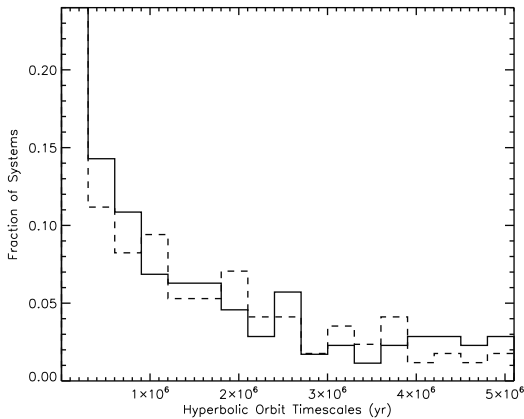


FIG. 8.— Histogram of times at which a planet first traveled on a hyperbolic orbit. The planets were evolved for 5 Myr. HNbody simulations are represented by solid lines and Hermite simulations are represented by dashed lines.

5. DISCUSSION

Forthcoming missions that promise to detect terrestrial planets within the habitable zone – such as *Kepler* – will also open the possibility of studying statistically the influence of massive planets on terrestrial planet formation (at least in the limited cases in which radial velocity surveys prove sensitive enough to constrain the giant planet populations around typically rather faint stars). That the existence of Jupiter and Saturn affects the formation of Earth and the rest of the inner Solar System, particularly in the vicinity of the asteroid belt, is well-established (Wetherill 1992; Lecar & Franklin 1997; Chambers & Cassen 2002; Levison & Agnor 2003; Mardling & Lin 2004). The distribution of extrasolar planetary masses is securely predicted to show a similar bimodality (Ida & Lin 2004, e.g.), due to the rapid timescale on which runaway accretion of giant planet envelopes occurs (Pollack et al. 1996), so a coupling between the observed properties of the giant and terrestrial planets in the same system is expected. Since giant extrasolar planets have substantially different orbital properties (and, perhaps, evolutionary histories) than those planets in the Solar System, we have argued here that the coupling between giant and terrestrial planet formation might be atypically weak in the Solar System, and more dramatic in extrasolar planetary systems.

The orbital properties of giant extrasolar planets immediately suggest two new mechanisms via which the evolution of giant planets might impede terrestrial planet formation. First, the orbital migration that is believed to be necessary to explain the origin of Hot Jupiters (Lin, Bodenheimer & Richardson 1997), and possibly the Late Heavy Bombardment

(Gomes et al. 2005), means that, at least in some systems and possibly in the typical system (Armitage et al. 2002; Trilling, Lunine & Benz 2002), giant planets move through the entire terrestrial planet zone during the early evolution of the disk. This may reduce the probability of subsequent terrestrial planet formation (Armitage 2003), though the extent of any suppression will depend on the speed of migration (which alters the degree of shepherdian via resonant capture) and on the surface density of planetesimals in the inner regions following scattering by the migrating planet (Ward & Hahn 1995; Tanaka & Ida 1999; Mandell & Sigurdsson 2003; Edgar & Artymowicz 2004; Raymond, Quinn & Lunine 2005; Fogg & Nelson 2005). EGPs which accrete onto the star may elongate the dynamical relaxation time of the planetesimal density distribution, and may occur repeatedly, further inhibiting terrestrial planet formation. Second, the large mean eccentricities of known giant extrasolar planets may signal that the typical planetary system is initially dynamically crowded and unstable to eventual gravitational scattering and planetary ejection. If this is the origin of eccentricity, then transient incursions by the giant planets into the terrestrial planet during the scattering process can be particularly detrimental to terrestrial planet formation, since the scattering is likely to occur at a relatively late epoch when the gas disk (which would tend to recircularize scattered planetesimals) has been dissipated. Studies of the dynamical stability of hypothetical terrestrial planets in known extrasolar planetary systems, which are normally based on presently observed pericenter values, may then hide the extent to which planets have swept out terrestrial material earlier in the history of that system (Veras & Armitage 2005).

In this paper, we have attempted to quantify – within a specific scattering scenario – the extent (in radius) of the anti-correlation this mechanism would introduce between the presence of giant and terrestrial planets in the same system. We find that during evolutionary sequences that end in plausible-looking planetary systems, one massive planet sweeps inward to less than half of the final (‘stable’) periastron distance approximately 30% of the time. Some effect persists (at the 10% level) down to orbital radii as small as 20% of the final periastron distance. If these simulations reflect the physical processes taking place in the early history of real extrasolar planetary systems, we predict that terrestrial planets ought to be under-abundant in nominally dynamically stable orbits interior to eccentric massive planets.

We thank an anonymous referee for constructive comments, and Hal Levison and Re'em Sari for valuable discussions. This work was supported by NASA under grants NAG5-13207, NNG04GL01G and from the Origins of Solar Systems and Astrophysics Theory Programs, and by the NSF under grant AST 0407040.

REFERENCES

- Adams, F. C., & Laughlin, G. 2003, *Icarus*, 163, 290
 Agol, E., Steffen, J.; Sari, R., Clarkson, W. 2005
 Armitage, P.J. 2003, *ApJ*, 582, L47
 Armitage, P. J., Livio, M., Lubow, S. H., & Pringle, J. E. 2002, *MNRAS*, 334, 248
 Artymowicz, P., Clarke, C. J., Lubow, S. H., & Pringle, J. E. 1991, *ApJ*, 370, L35
 Asghari, N., et al. 2004, *A&A*, 426, 353
 Basri, G., Borucki, W. J., & Koch, D. 2005
 Bennett, D.P., Rhie, S.H. 2002 *ApJ*, 574, 985
 Chambers, J.E., Cassen, P. 2002, *Meteoritics & Planetary Science*, 37, 1523
 Chambers, J.E., Wetherill, G.W., Boss, A.P. 1996, *Icarus*, 119, 261
 Cumming, A. 2004, *MNRAS*, 354, 1165

- Edgar, R., & Artymowicz, P. 2004, MNRAS, 354, 769
- Fogg, M. J., Nelson, R. P. 2005, A&A, 441, 791.
- Ford, E. B., Havlickova, M., & Rasio, F. A. 2001, Icarus, 150, 303
- Ford, E. B., Lystad, V., Rasio, F. A. 2005, Nature, 434, 873
- Ford, E. B., Rasio, F. A., & Yu, K. 2003, in "Scientific Frontiers in Research on Extrasolar Planets", ASP Conf. Ser. Vol 294, eds D. Deming and S. Seager (San Francisco: ASP), p. 181
- Ford, E.B., Tremaine, S. 2003, PASP, 812, 1171
- Franklin, F. A., Lewis, N. K., Soper, P. R., & Holman, M. J. 2004, AJ, 124, 1391
- Goldreich, P., Lithwick, Y., & Sari, R. 2004, ARA&A, 42, 549
- Goldreich, P., & Sari, R. 2003, ApJ, 585, 1024
- Gomes, R., Levison, H.F., Tsiganis, K., & Morbidelli, A. 2005, Nature, 435, 466
- Hahn, J. M., & Malhotra, R. 1999, AJ, 117, 3041
- Haisch, K. E., Jr., Lada, E. A., & Lada, C. J. 2001, ApJ, 553, L153
- Holman, M. J., & Wisdom, J. 1993, AJ, 105, 1987
- Holman, M. J., & Murray, N. W. 2005, Science, 307, 1288
- Hut, P., & Makino, J. 2003, in "The Art of Computational Science"
- Ida, S., Lin, D.N.C. 2004, ApJ, 604, 388
- Ito, T., Tanikawa, K. 2001, PASJ, 53, 143
- Ji, J., Liu, L., Kinoshita, H., Li, G. 2005, ApJ, 631, 1191
- Jones, B. W., Sleep, P. N., & Chambers, J. E. 2001, A&A, 366, 254
- Lecar, M., & Franklin, F. 1997, 129, 134
- Levison, H. F., Lissauer, J. J., & Duncan, M. J. 1998, AJ, 116, 1998
- Levison, H. F., & Agnor, C. 2003, AJ, 125, 2692
- Lin, D. N. C., Bodenheimer, P., & Richardson, D. C. 1997, Nature, 380, 606
- Lin, D. N. C., & Ida, S. 1997, ApJ, 477, 781
- Malhotra, R. 1995, AJ, 110, 420
- Mandell, A. M., & Sigurdsson, S. 2003, ApJ, 599, L111
- Mardling, R.A., Lin, D.N.C. 2004, ApJ, 614, 955
- Marzari, F., & Weidenschilling, S. J. 2002, Icarus, 156, 570
- Menou, K., Tabachnik, S. 2003, ApJ, 583, 473
- Murray-Clay, R. A., & Chiang, E. I. 2005, ApJ, 619, 623
- Ogilvie, G. I., & Lubow, S. H. 2003, ApJ, 587, 398
- Papaloizou, J. C. B., Nelson, R. P., & Masset, F. 2001, A&A, 366, 263
- Papaloizou, J. C. B., & Terquem C. 2001, MNRAS, 325, 221
- Pollack, J. B., Hubickyj, O., Bodenheimer, P., Lissauer, J. J., Podolak, M., & Greenzweig, Y. 1996, Icarus, 124, 62
- Rasio, F. A., & Ford, E. B. 1996, Science, 274, 954
- Raymond, S.N., Quinn, T., & Lunine, J.I. 2005, Icarus, 177, 256.
- Tabachnik, S., Tremaine, S. 2002, MNRAS, 335, 151
- Tanaka, H., & Ida, S. 1999, Icarus, 139, 350
- Thommes, E. W., Duncan, M. J., & Levison, H. F. 1999, Nature, 402, 635
- Thommes, E. W., Duncan, M. J., & Levison, H. F. 2002, AJ, 123, 2862
- Trilling, D. E., Lunine, J. I., & Benz, W. 2002, A&A, 394, 241
- Tsiganis, K., Gomes, R., Morbidelli, A., & Levison, H. F. 2005, Nature, 435, 459
- Veras, D., Armitage, P. J. 2004a MNRAS, 347, 613
- Veras, D., Armitage, P. J. 2004b Icarus, 172, 349
- Veras, D., Armitage, P. J. 2005 ApJL, 620, L111
- Ward, W. R., & Hahn, J. M. 1995, ApJ, 440, L25
- Wetherill, G. W. 1992, Icarus, 100, 307
- Wisdom, J. 1980, AJ, 85, 1122
- Wolk, S. J., & Walter, F. M. 1996, AJ, 111, 2066
- Zhang, K., Hamilton, D. 2005 DDA #36, #11.06